


Review

Residual Strength Assessment and Residual Life Prediction of Corroded Pipelines: A Decade Review

Haotian Li ¹, Kun Huang ^{1,*}, Qin Zeng ² and Chong Sun ³

¹ School of Petroleum and Natural Gas Engineering, Southwest Petroleum University, Chengdu 610500, China; 20222000803@stu.swpu.edu.cn

² PetroChina Southwest Oil and Gas Field Gas Branch, Chengdu 610500, China; zengqin01@petrochina.com.cn

³ Sinopec Petroleum Engineering Zhongyuan Corporation, Puyang 457000, China; sunch.osec@sinopec.com

* Correspondence: hkswp@swpu.edu.cn

Abstract: Prediction of residual strength and residual life of corrosion pipelines is the key to ensuring pipeline safety. Accurate assessment and prediction make it possible to prevent unnecessary accidents and casualties, and avoid the waste of resources caused by the large-scale replacement of pipelines. However, due to many factors affecting pipeline corrosion, it is difficult to achieve accurate predictions. This paper reviews the research on residual strength and residual life of pipelines in the past decade. Through careful reading, this paper compared several traditional evaluation methods horizontally, extracted 71 intelligent models, discussed the publishing time, the evaluation accuracy of traditional models, and the prediction accuracy of intelligent models, input variables, and output value. This paper's main contributions and findings are as follows: (1) Comparing several traditional evaluation methods, PCORRC and DNV-RP-F101 perform well in evaluating low-strength pipelines, and DNV-RP-F101 has a better performance in evaluating medium–high strength pipelines. (2) In intelligent models, the most frequently used error indicators are mean square error, goodness of fit, mean absolute percentage error, root mean square error, and mean absolute error. Among them, mean absolute percentage error was in the range of 0.0123–0.1499. Goodness of fit was in the range of 0.619–0.999. (3) The size of the data set of different models and the data division ratio was counted. The proportion of the test data set was between 0.015 and 0.4. (4) The input variables and output value of predictions were summarized.

Keywords: residual strength; residual life; evaluation criterion; intelligent model



Citation: Li, H.; Huang, K.; Zeng, Q.; Sun, C. Residual Strength Assessment and Residual Life Prediction of Corroded Pipelines: A Decade Review. *Energies* **2022**, *15*, 726. <https://doi.org/10.3390/en15030726>

Academic Editors: Xin Ma, Xiaoben Liu, Pei Du and Jingwei Cheng

Received: 14 December 2021

Accepted: 15 January 2022

Published: 19 January 2022

Publisher's Note: MDPI stays neutral with regard to jurisdictional claims in published maps and institutional affiliations.



Copyright: © 2022 by the authors. Licensee MDPI, Basel, Switzerland. This article is an open access article distributed under the terms and conditions of the Creative Commons Attribution (CC BY) license (<https://creativecommons.org/licenses/by/4.0/>).

1. Introduction

The pipeline is the primary transportation mode of oil and gas, which also accounts for a considerable proportion of the national economy, and the safe operation of pipelines is also closely related to people's lives. Due to the vast area, complex geology, different soil properties, and significant differences in a corrosive environment, pipelines are very vulnerable to external corrosion, which reduces their safety and service life. Pipeline leakage is one of the most critical potential safety hazards of long-distance oil and gas pipeline transportation.

According to the 11th EGIG report [1], incidents caused by corrosion accounted for 26% during the period 2009–2013 and 24% during the period 2004–2013, and the incidents caused by corrosion accounted for 26.63% during the period 2010–2019. The incidents with leak size pinhole/crack caused by corrosion accounted for 38% (Figure 1).

With the frequent accidents caused by corroded pipelines, it is still necessary to do more research on pipeline residual strength evaluation and residual life prediction. The significance of residual strength evaluation and residual life prediction has two aspects: (a) accurate assessment and prediction makes it possible to prevent unnecessary accidents and casualties; (b) accurate assessment and prediction can avoid the waste of resources

caused by the large-scale replacement of pipelines through repairing it in advance. Therefore, residual strength assessment and residual life prediction have attracted a large number of scholars, and due to the popularity of artificial intelligence and machine learning in recent years; a large number of scholars use intelligent models as their research methods. For example, we search the literature in the ScienceDirect database with the following requirements: (1) Search target: "residual strength assessment" or "residual life prediction"; (2) Period: 2009–2021; (3) Article type: "Review articles" and "Research articles". A total 168 papers were retrieved.

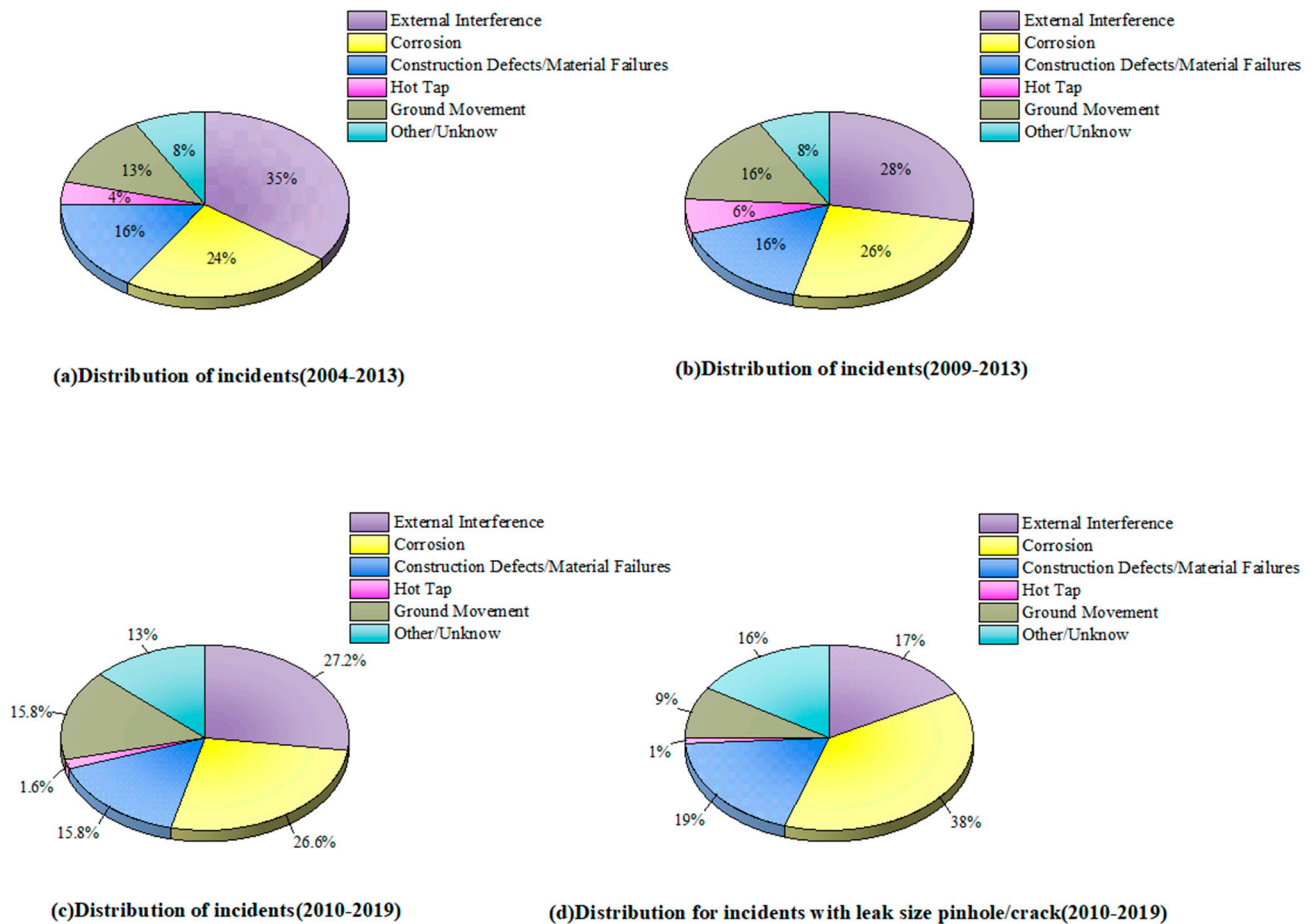


Figure 1. Distribution of incidents: (a) 2004–2013; (b) 2009–2013; (c) 2010–2019; (d) with leak size pinhole/crack (2010–2019).

These papers can be roughly divided into the evaluation of traditional methods and the prediction of intelligent models. Most of the research based on traditional methods has been performed well, but in the research using intelligent models, researchers can only compare the basic models with the improved models, due to their limited energy, and there is no more comprehensive review to compare a large number of intelligent models. The purposes of this paper are to:

1. Provide selection reference for researchers;
2. Compare the advantages and disadvantages of the methods to help researchers understand each method;
3. Provide a reference for future research.

The rest of this paper is organized as follows: Section 2 introduces the literature review methodology. Section 3 reviews the prediction models and methods, and classifies them according to traditional methods and intelligence methods. Section 4 discusses the

applicable conditions of traditional methods, compares the prediction accuracy under different pipe steel grades, and reviews the model, data size, input variable, output value, publishing time, performance of intelligent methods, and the future research directions. Section 5 summarizes the primary conclusions of this paper.

2. Methodology

The methodology of this review is summarized as follows, mainly including four steps:

- Step 1: Multiple database searches.

According to our preliminary search results, there is not enough quantity in a single database. In order to summarize more comprehensively and have more reference value, we have combined the search results of multiple databases. The critical information of the search is as follows:

Object: residual life/strength prediction of corroded pipeline.

Database: Google Scholar, Web of Science, ASCE, SPE, ScienceDirect, CNKI.

Keywords: residual strength, residual life, evaluation method, intelligent model.

Language: English.

Period: 2009–2021

- Step 2: Review and screening.

In the collected literature, many are related to the residual strength evaluation and residual life prediction, but the experimental object is not the corroded pipeline. In order to achieve better results and determine that the content is directly related to the residual life prediction and residual strength evaluation of the corroded pipeline, we read each paper carefully.

- Step 3: Extracting information from papers.

Read the paper in-depth and extract meaningful information, such as the utilized model, prediction accuracy, data size, proportion of test data set, input variables, and output value.

- Step 4: Discussion and conclusion.

Discuss the information extracted in step 3, make a comprehensive review, summarize the existing research, and put forward possible research directions in the future.

3. Literature Review

3.1. Traditional Evaluation Methods

3.1.1. ASME B31G-1984

In the late 1960s, Texas Eastern transportation company and American Natural Gas Association (AGA) conducted relevant research on corroded pipelines and proposed NG-18 formula [2]. All subsequent formulas of this series evolved from it, and the expression is shown in Equation (1).

$$P_f = \sigma_{flow} \left(\frac{1 - \frac{A}{A_0}}{1 - \frac{A}{A_0} \frac{1}{M}} \right) \quad (1)$$

In 1984, ASME B31G-1984, as the earliest residual strength evaluation criterion of corroded pipelines [3], was proposed by American Society of Mechanical Engineers based on NG-18. The specific parameters in NG-18 formula were given. $\frac{l^2}{Dt} \leq 20$ is defined as a short defect and $\frac{l^2}{Dt} \geq 20$ is defined as a long defect. According to different defect length, there are two formulas for calculating failure pressure of pipeline (Equation (2)).

$$P_f = \sigma_{flow} \left(\frac{1 - \frac{A}{A_0}}{1 - \frac{A}{A_0} \frac{1}{M}} \right) \quad (2)$$

3.1.2. ASME B31G-1991

In 1991, American Society of Mechanical Engineers had made some modifications to B31G-1984, and proposed ASME B31G-1991 [4]. The new criterion retained the original flow stress, and modified the Folias bulging coefficient and the calculation formula of long defect failure pressure, the expression is shown in Equation (3).

$$P_f = \frac{\sigma_{flow} 2t}{D} \left(1 - \frac{d}{t} \right) \quad (3)$$

Compare to B31G-1984, the results of B31G-1991 evaluation criterion is less conservative.

3.1.3. Modified B31G

Kiefner and others of the American Natural Gas Association (AGA) [5] found that improper definition of flow stress, inaccurate expression of the Folias bulging coefficient, and inaccurate calculation of metal loss area caused B31G-1984 to be too conservative. In view of the above problems, Kiefner and his colleagues proposed the modified B31G criterion. The modified evaluation criterion does not distinguish the size of defects when simplifying the projected area of defect profile, but takes $A = 0.85 dL$. Therefore, this evaluation method is also called "RSTRENG 0.85 dL evaluation method". The expression of failure pressure is shown in Equation (4).

$$P_f = \frac{\sigma_{flow} 2t}{D} \left(\frac{1 - 0.85 \frac{d}{t}}{1 - 0.85 \frac{d}{t} \frac{1}{M}} \right) \quad (4)$$

3.1.4. ASME B31G-2009

Based on the previous two editions of ASME B31G, the criterion was revised again in 2009 and ASME B31G-2009 was obtained [6]. This version adopts the concept of hierarchical evaluation for the first time (Figure 2). The higher the evaluation level, the more accurate the evaluation result. However, the difficulty of evaluation also increases [7]. Therefore, different levels of the evaluation methods should be selected according to the actual situation in the application.

1. Zero-level evaluation

According to the collected corrosion defect parameters and pipeline parameters, query the table to obtain the maximum allowable length of this defect. If the actual corrosion length is less than the maximum longitudinal length, it is safe; otherwise, it fails to pass the evaluation. At this time, maintenance measures shall be taken, or a higher-level evaluation method shall be selected. The zero-level evaluation is simple to use, but the results are conservative.

2. First-level evaluation

First, calculate the failure pressure of the corroded pipeline by the Modified B31G method, and then compare it with the product of the pipeline safety factor and the operating pressure for evaluation. The first-level evaluation needs to be completed by professionals such as corrosion technicians or coating inspectors.

3. Second-level evaluation

The criterion recommends that the second-level evaluation use the RSTRENG effective area method to evaluate the residual strength of corroded pipelines. The effective area method has a wide range of applications, and it is also applicable to independent defects and interacting defect groups. However, it also has certain limitations. The effective area calculation requires a detailed measurement of the defect size, and software is also required, so it is rarely used in actual working conditions.

4. Third-level evaluation

It is recommended to use the finite element analysis method for stress analysis of the corroded pipeline. The finite element analysis method is a mathematical simulation method, which calculates the bearing capacity of the pipeline by considering many factors such as the real stress–strain curve of material, actual load, boundary conditions, and so on. The evaluation process is more cumbersome, but the results are more accurate.

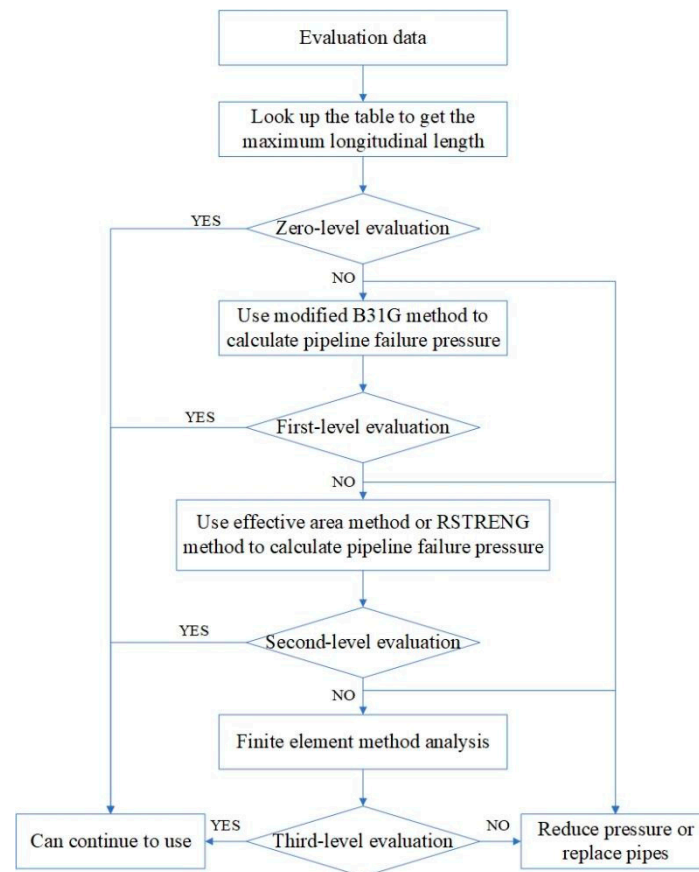


Figure 2. The evaluation process of ASME B31G-2009.

3.1.5. DNV-RP-F101

In 1999, British Gas Company (BG) and DET NORSKE VERITAS (DNV) jointly developed the specification for the evaluation of pipelines with corrosion defects, namely, DNV-RP-F101 [8]. The DNV-RP-F101 criterion provides two evaluation criteria: partial safety factor and allowable stress [9]. The main difference between the two evaluation methods lies in the different safety criteria.

1. Partial safety factor method

The partial safety factor method is a set of safety guidelines based on the DNV offshore criterion OS-F101 and the submarine pipeline system, which fully considers uncertain factors such as the depth of corrosion defects and material properties. The calculation formula of failure pressure is shown in Equation (5).

$$P_f = \gamma_m \frac{2t\sigma_u}{D-t} \frac{1 - \gamma_d \left(\frac{d}{t}\right)^*}{1 - \frac{\gamma_d \left(\frac{d}{t}\right)^*}{M}} \quad (5)$$

2. Allowable stress method

The allowable stress method is a safety criterion design based on allowable stress. It does not consider many complicated factors. The calculation is simple but not as objective

and accurate as the partial safety factor method. The calculation formula of failure pressure is shown in Equation (6).

$$P_f = \frac{\sigma_u 2t}{D-t} \left(\frac{1 - \frac{d}{t}}{1 - \frac{d}{t} \frac{1}{M}} \right) \quad (6)$$

3.1.6. PCORRC

PCORRC (Pipeline Corrosion Criterion) [10] is a recent evaluation method mainly used to evaluate the residual strength of the medium and high strength steel pipes with blunt corrosion defects due to plastic instability. This method is obtained by Stephens using shell elements to simulate corrosion defects. In this method, the failure pressure of pipelines is determined by tensile strength, not yield strength or flow stress. The calculation formula of failure pressure is shown in Equation (7).

$$P_f = \frac{\sigma_u 2t}{D-t} \left\{ 1 - \frac{d}{t} \left[1 - \exp \left(\frac{-0.157l}{\sqrt{\frac{Dt-Dd}{2}}} \right) \right] \right\} \quad (7)$$

The failure pressure calculation formula is obtained by fitting the finite element calculation results, mainly considering defects' length and depth.

3.1.7. RSTRENG

On the basis of ASME B31G-1991, Kiefner and Vieth developed the RSTRENG calculation program, called RSTRENG [11] method, by redefining the Folias factor and material flow stress, and describing the shape of corrosion defects in more detail. RSTRENG is mainly used to evaluate the residual strength of externally corroded pipelines, including RSTRENG 0.85-area method and RSTRENG effective area method [12].

1. RSTRENG 0.85-area method

RSTRENG only requires two parameters: defect depth and length, but adds the flow stress value defined in ASME B31G. In contrast, ASME B31G is more conservative than RSTRENG 0.85-area method, and is the same as the modified B31G in the definitions of flow stress, Folias factor, and defect projection area. The calculation formula is shown in Equation (8).

$$P_f = \frac{\sigma_{flow} 2t}{D} \left(\frac{1 - 0.85 \frac{d}{t}}{1 - 0.85 \frac{d}{t} \frac{1}{M}} \right) \quad (8)$$

2. RSTRENG effective area method

The RSTRENG effective area evaluation method requires defect depth, defect length, data along the axial and circumferential directions of defects, and detailed corrosion profile. The calculation of the effective area is closer to the actual results. The effective area method has higher accuracy, but the calculation is more complex. The calculation formula is shown in Equation (9).

$$P_f = \frac{\sigma_{flow} 2t}{D} \left(\frac{1 - \frac{A}{A_0}}{1 - \frac{A}{A_0} \frac{1}{M}} \right) \quad (9)$$

3.1.8. Others

In addition to the above evaluation methods, there are still some other evaluation methods, such as SY/T 6151-2009 [13] and BS 7910-2005 [14]. SY/T 6151-2009 "evaluation method for corrosion damage of steel pipeline" is the latest oil and gas industry criterion of China issued in December 2009. Compared with ASME B31G criterion, SY/T 6151 criterion considers the influence of circumferential corrosion length, applies fracture mechanics theory to determine the maximum safe working pressure, and classifies and evaluates according to the degree of pipeline corrosion damage. The BS7910-2005 method divides

corrosion defects into single defects and combined defects, and uses tensile strength instead of flow stress in the calculation formula.

3.1.9. Comparison

Several existing main residual strength evaluation criteria for corroded pipelines are introduced above, including ASME B31G, modified B31G, DNV-RP-F101, RSTRENG, etc. The above methods have different formula definitions, bulging coefficient and defect area, and their application scope, applicable defect type, and load type are different. The comparison of main criteria and methods is shown in Tables 1 and 2.

Table 1. Comparison of parameters in residual strength evaluation methods.

Evaluation Method	Flow Stress	Folias Bulging Coefficient	Corrosion Projection Area
ASME B31G	1.1SMYS	$M = \sqrt{1 + \frac{0.8l^2}{Dt}}$	$\frac{2}{3}dl$ (parabolic); dl (rectangle).
Modified B31G	SMYS + 68.95	$M = \begin{cases} \sqrt{1 + 0.6275\left(\frac{l}{\sqrt{Dt}}\right)^2 - 0.003375\left(\frac{l}{Dt}\right)^4} & \left(\frac{l^2}{Dt} \leq 50\right) \\ 0.032\frac{l^2}{Dt} + 3.3 & \left(\frac{l^2}{Dt} \geq 50\right) \end{cases}$	$0.85dl$ (between parabolic and rectangle)
SY/T 6151-2009	SMTS + 68.95	$M = \begin{cases} \sqrt{1 + 0.6275\left(\frac{l}{\sqrt{Dt}}\right)^2 - 0.003375\left(\frac{l}{Dt}\right)^4} & \left(\frac{l^2}{Dt} \leq 50\right) \\ 0.032\frac{l^2}{Dt} + 3.3 & \left(\frac{l^2}{Dt} \geq 50\right) \end{cases}$	$0.85dl$ (between parabolic and rectangle)
DNV-RP-F101	SMTS	$M = \sqrt{1 + 0.31\left[\frac{l}{\sqrt{Dt}}\right]^2}$	dl
PCORRC	SMTS	—	—
RSTRENG	SMTS + 68.95	$M = \begin{cases} \sqrt{1 + 0.6275\left(\frac{l}{\sqrt{Dt}}\right)^2 - 0.003375\left(\frac{l}{Dt}\right)^4} & \left(\frac{l^2}{Dt} \leq 50\right) \\ 0.032\frac{l^2}{Dt} + 3.3 & \left(\frac{l^2}{Dt} \geq 50\right) \end{cases}$	$0.85dl$ (between parabolic and rectangle)
0.85-area method	SMTS + 68.95	$M = \begin{cases} \sqrt{1 + 0.6275\left(\frac{l}{\sqrt{Dt}}\right)^2 - 0.003375\left(\frac{l}{Dt}\right)^4} & \left(\frac{l^2}{Dt} \leq 50\right) \\ 0.032\frac{l^2}{Dt} + 3.3 & \left(\frac{l^2}{Dt} \geq 50\right) \end{cases}$	—
RSTRENG Effect area method	SMTS + 68.95	$M = \begin{cases} \sqrt{1 + 0.6275\left(\frac{l}{\sqrt{Dt}}\right)^2 - 0.003375\left(\frac{l}{Dt}\right)^4} & \left(\frac{l^2}{Dt} \leq 50\right) \\ 0.032\frac{l^2}{Dt} + 3.3 & \left(\frac{l^2}{Dt} \geq 50\right) \end{cases}$	—

Table 2. Comparison of residual strength evaluation methods for pipes with different corrosion defect.

Evaluation Method	Best Scope of Application	Defect Type	Load Type
ASME B31G	Medium and low strength steel	Isolated defect	Internal pressure
Modified B31G	Medium and low strength steel	Isolated defect or treat the interaction defect as an isolated defect	Internal pressure
SY/T 6151-2009	Carbon steel and low alloy steel pipes with blunt and low stress concentration corrosion damage	Isolated defect or treat the interaction defect as an isolated defect	Internal pressure
DNV-RP-F101	Medium and high strength steel	Single defect/interaction defect, complex shape defect	Internal pressure/axial compressive stress
PCORRC	Medium and high strength steel	Isolated defect or treat the interaction defect as an isolated defect	Internal pressure
RSTRENG Effect area	Medium and low strength steel	Complex shape defect	Internal pressure

3.2. Intelligent Methods

In the actual pipeline transportation system, many influencing factors do not have a clear functional relationship, and the practical application effect of traditional methods is often not ideal. Therefore, some intelligent methods are gradually used in the field of pipeline corrosion prediction, such as fuzzy mathematics theory method, artificial neural network method, chaos theory method, support vector machine, and so on.

3.2.1. ANN

Deep learning is a branch of machine learning, and ANN is a neural network in deep learning. ANN builds mathematical models by abstracting, simplifying, and simulating biological neural networks' structure and operating mechanism to process information [15]. A large number of biological neurons connects biological neural networks. Similarly, ANN is also composed of multiple neurons connected according to certain rules. Figure 3 below shows an artificial neural network [16].

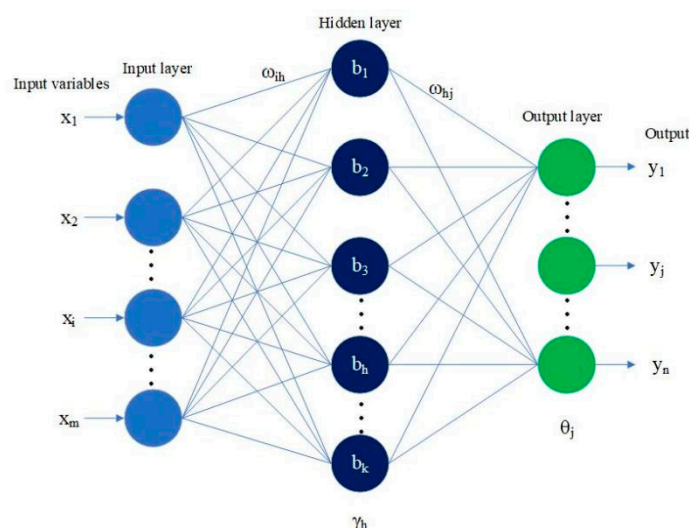


Figure 3. Neural network structure.

In Figure 3, the neural network includes input layer, hidden layer, and output layer. Suppose a training sample is $x = (x_1, x_2, x_3, \dots, x_m) \in R_m$, the corresponding output vector is $y = (y_1, \dots, y_n)$, and n is the number of categories. Each neuron has a weight. The input weight of the n th node of the hidden layer is $\omega_{1h}, \omega_{2h}, \dots, \omega_{mh}$, and the corresponding offset is γ_h . The input weight of the j th output layer node is $\omega_{1j}, \omega_{2j}, \dots, \omega_{kj}$, and the corresponding offset is θ_j . k is the number of hidden layer nodes. In addition, the hidden layer can be multiple layers.

According to Figure 3, the input of the j th output neuron is shown in Equation (10).

$$\beta_j = \sum_{h=1}^k \omega_{hj} b_h \quad (10)$$

The output of the j th output neuron is shown in Equation (11).

$$y_j = f(\beta_j + \theta_j) \quad (11)$$

The input of the h th hidden layer neuron is shown in Equation (12).

$$\alpha_h = \sum_{i=1}^m \omega_{ih} x_i \quad (12)$$

The output of the h th hidden layer neuron is shown in Equation (13).

$$b_h = f(\alpha_h + \gamma_h) \quad (13)$$

In recent years, a growing number of researchers has been using ANN in the oil and gas industry [17], including predicting the remaining strength and remaining life of corroded pipelines. The basic idea of its application is to collect and sort out the pipeline data and then use the built model to train the data set. ANN can better perceive the

nonlinear relationship between corrosion factors and corrosion rate to accurately predict the corrosion trend (Figure 4).

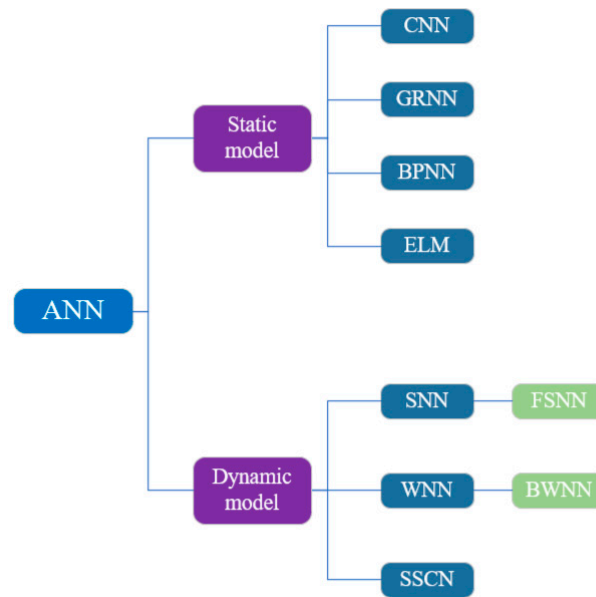


Figure 4. Nine ANN-based models for residual strength or residual life prediction.

Artificial neural networks have many advantages. For example, they can learn any nonlinear function, and artificial neural networks can learn the weights that map any input to output. It also faces some challenges, such as slow training when there is a lot of data, many parameters, and weak interpretability.

3.2.2. Fuzzy Mathematics

Aiming at the randomness and fuzziness of the system, it judges and extracts the uncertainty of the system according to the theory and method of fuzzy mathematics to achieve the purpose of analyzing the system. In short, it is an evaluation method that uses the membership theory of fuzzy mathematics to transform the qualitative evaluation of objects affected by many factors into quantitative evaluation to clarify the fuzzy phenomenon.

1. Triangular fuzzy mathematics theory.

In Figure 5, m is the kernel of A^* ; $u + l$ is the blindness of A^* ; u is the membership function of the triangular fuzzy number; A^* is the triangular fuzzy number, denoted as $A^* = (l_{ij}, m_{ij}, u_{ij})$.

$$\mu_{A^*}(x) = \begin{cases} (x - m + l)/l, & l \leq x \leq m \\ (m + u - x)/u, & m \leq x \leq u \\ 0, & \text{others} \end{cases} \tag{14}$$

The triangular fuzzy number $A^* = (l_{ij}, m_{ij}, u_{ij})$ is used to represent the judgment result of the importance of evaluation factor μ_i to evaluation factor μ_j . Among them, m_{ij} is the possible value of measuring the result, which is generally determined by the 1–9 scale method shown in Table 3. l and u represent fuzzy degree. The larger the $u-l$, the stronger the fuzzy degree. The importance of μ_j to μ_i is shown in Equation (15).

$$A^*_{ji} = A^*_{ij}' = (1/l_{ij}, 1/m_{ij}, 1/u_{ij}) \tag{15}$$

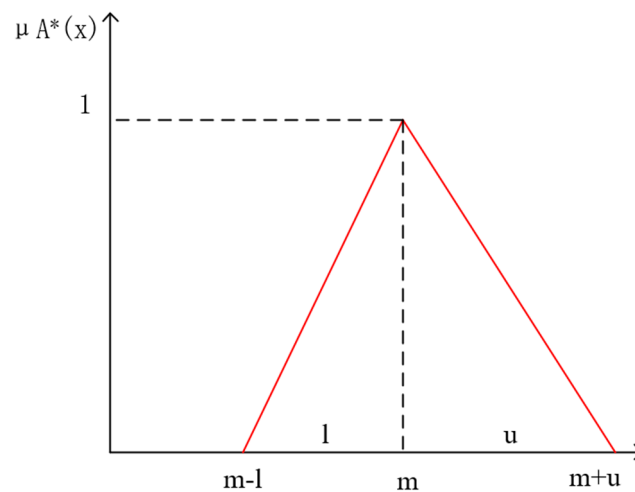


Figure 5. Membership function curve of triangular fuzzy number [18].

Table 3. Scale method [19].

Scale	Relative Comparison
1	Two factors are equally important
3	One factor is slightly more important than the other
5	One factor is obviously more important than another
7	One factor is obviously much more important than another
9	One factor is absolutely more important than another
2,4,6,8	The importance is between 1.3.5.7.9

Assuming that the fuzzy numbers q_1 and q_2 are represented by parameters (l_1, m_1, u_1) and (l_2, m_2, u_2) , respectively, the algebraic operation law of triangular fuzzy numbers q_1 and q_2 can be expressed as Equation (16).

$$\begin{cases} q_1 \oplus q_2 = (l_1, m_1, u_1) \oplus (l_2, m_2, u_2) = (l_1 + l_2, m_1 + m_2, u_1 + u_2) \\ q_1 - q_2 = (l_1, m_1, u_1) - (l_2, m_2, u_2) = (l_1 - l_2, m_1 - m_2, u_1 - u_2) \\ q_1 \otimes q_2 = (l_1, m_1, u_1) \otimes (l_2, m_2, u_2) = (l_1 l_2, m_1 m_2, u_1 u_2) \\ C \otimes q_1 = (Cl_1, Cm_1, Cu_1) \end{cases} \quad (16)$$

- Establish unit fuzzy judgment matrix.

Suppose there are t objects, and the k th ($k = 1, 2, \dots, t$) object is compared in pairs for n factors in turn (as long as $n(n - 1)/2$ times), the unit fuzzy judgment matrix is obtained (Equation (17)).

$$A^{(k)} = (A^*)_{n \times n} \quad (17)$$

where $(A^*) = (l_{ij}^{(k)}, m_{ij}^{(k)}, u_{ij}^{(k)})$.

- Aggregate unit fuzzy judgment matrix.

According to the specific conditions of the t factors, the weight r_k is given respectively, and then their respective unit fuzzy judgment matrix seasons can be changed to the fuzzy judgment matrix A^* by the operation rules of triangular fuzzy numbers, and its elements (Equation (18))

$$A^* = (l_{ij}, m_{ij}, u_{ij}) = \frac{1}{\sum_{k=1}^t r_k} \left[\sum_{k=1}^t (l_{ij}^{(k)}, m_{ij}^{(k)}, u_{ij}^{(k)}) \cdot r_k \right] \quad (18)$$

2. General steps of fuzzy comprehensive evaluation method [20].

- Establish factor set $X = (X_1, X_2, \dots, X_i)$, which is composed of evaluation indexes; Construct weight vector $A = (a_1, a_2, \dots, a_i)$. Define the comment set as $W = (w_1, w_2, \dots, w_i)$, and obtain the corresponding weight set Y of the factor set $Y = (Y_1, Y_2, \dots, Y_i)$.
- Construct weight vector $A = (a_1, a_2, \dots, a_i)$.
- Construct evaluation matrix (Equation (19)).

$$R = \begin{bmatrix} r_{11} & r_{12} & \dots & r_{1j} \\ r_{21} & r_{22} & \dots & r_{2j} \\ \dots & \dots & \dots & \dots \\ r_{i1} & r_{i2} & \dots & r_{ij} \end{bmatrix} \quad (19)$$

where r_{xy} ($x = 1, 2, \dots, i; y = 1, 2, \dots, j$) represents the degree of membership of the factor level index X_x to the y th comment set w_y .

- Calculate fuzzy matrix.

Obtain the membership vector B of the factor layer index to the comment set (Equation (20)):

$$B = YR = (Y_1, Y_2, \dots, Y_i) \begin{bmatrix} r_{11} & r_{12} & \dots & r_{1j} \\ r_{21} & r_{22} & \dots & r_{2j} \\ \dots & \dots & \dots & \dots \\ r_{i1} & r_{i2} & \dots & r_{ij} \end{bmatrix} = (b_1, b_2, \dots, b_j) \quad (20)$$

when $\sum_{x=1}^j b_x \neq 1$, let $b^*_x = b_x / \sum_{x=1}^j b_x$ to obtain (Equation (21)):

$$B^* = (b^*_1, b^*_2, \dots, b^*_j) \quad (21)$$

where B^* is the membership vector of target layer index x to comment set W . According to the specific content of B^* , the corresponding evaluation can be obtained.

3.2.3. Chaos Theory and Method

In 1905, H. Poincare discovered chaos for the first time in his research and put forward the H. Poincare conjecture: a small error in the initial conditions produces a great error in the final phenomenon, so the prediction becomes impossible. In 1963, the American meteorologist Lorenz discovered in numerical experiments that deterministic systems sometimes exhibit random behavior phenomena, and then he called it "deterministic nonperiodic flow" in the literature [21]. In 1975, Li TY and Yorke gave a specific definition of chaos for the first time [22]: chaos is a kind of random and random phenomenon that occurs in a deterministic system and is sensitive to initial conditions. It is a phenomenon that exists widely in nature.

The mathematics model of Chaos:

- Collect a digital sequence $(x_0, x_1, x_2, \dots, x_i, \dots, x_s)$ of a certain characteristic quantity of the observed system.
- Using difference can generate new first-order difference sequence, second-order difference sequence... (Equations (22) and (23)).

$$\Delta x_n = x_{n+1} - x_n \quad (22)$$

$$\Delta(\Delta x) = \Delta^2 x \quad (23)$$

- Take the number of observations as the horizontal axis and the characteristic quantity as the vertical axis to make a graph, which can intuitively and qualitatively grasp the time structure and trend of the phenomenon change.
- Based on the prediction sequence, calculate any item with one or more items in front of the sequence by assuming the changing structure (Equation (24)):

$$x_{n+1} = f(x_n) = f(f(x_{n-1})) = f^2(x_{n-1}) = f^n(x_0) \quad (24)$$

Chaos theory is the analysis of irregular and unpredictable phenomena and processes. In essence, a chaotic process is a deterministic process, but it is disorderly, fuzzy, and random on the surface. This is similar to the corrosion development process of pipeline system, but the required sample size must be sufficient.

3.2.4. SVM

Support vector machine, which Cortes and Vapnik first proposed in 1995 [23], is a practical algorithm for nonlinear classification and regression problems in the case of small samples. When dealing with the regression problem, the basic idea is to map the low-dimensional nonlinear regression problem to the high-dimensional feature space, and establish a model in the high-dimensional feature space to learn the data set for regression fitting [24].

Using the basic idea of support vector machine, the data set (x_1, x_2, \dots, x_n) is mapped to a high-dimensional feature space, and then the data set X is used to establish a model in this space for linear regression. The regression form is as Equation (25).

$$f(x_i) = \omega \cdot \varphi(x_i) + b \quad (25)$$

where ω, b is regression factor, φ is the coefficient to be determined in the model.

In order to obtain the regression function, the above problem is transformed into the following planning problem (Equation (25)).

$$\min \frac{1}{2} \omega^T \omega + C \sum_{i=1}^n \xi_i + C \sum_{i=1}^n \xi_i^* \quad (26)$$

Constraints are:

$$\text{s.t.} \begin{cases} y_i - \omega \cdot \varphi(x_i) - b \leq \varepsilon + \xi_i^* \\ \omega \cdot \varphi(x_i) + b - y_i \leq \varepsilon + \xi_i \\ \xi_i, \xi_i^* \geq 0 \end{cases}$$

where C is the penalty term constant, ε is the insensitive loss function, and ξ_i, ξ_i^* are the slack variables.

By introducing Lagrange function, the above optimization problem can be transformed into Lagrange dual problem, and the solution is as follows:

$$f(x) = \sum_{i=1}^l (\alpha_i - \alpha_i^*) K(X_d, X) + b \quad (27)$$

where α_i, α_i^* is the Lagrange multiplier, when $(\alpha_i - \alpha_i^*)$ is not 0, the corresponding sample is support vector; $K(X_d, X)$ is the kernel function, the selection of kernel function should make it a point product of high-dimensional feature space.

SVM as a typical machine learning method, is widely used in classification and regression. It can avoid the neural network falling into local optimization, and it is usually used in the case of small amount of data such as pipeline corrosion failure.

3.2.5. Comparison

Choosing appropriate methods can effectively improve the evaluation effect and prediction accuracy. The advantages and disadvantages of each method are listed in Table 4 to facilitate researchers choosing and using a suitable method.

Table 4. Merits and limitations of various methods.

Methods	Merit	Limitation
ANN	It has strong robustness and fault tolerance to noise neural network, can fully approach complex nonlinear relations, and has the function of associative memory.	Neural network needs a large number of parameters and its interpretability is not strong.
Fuzzy mathematics	It is able to make a more scientific, reasonable, and realistic quantitative evaluation of the data with the hidden information presenting fuzziness. The evaluation result is a vector, not a point value. It contains rich information that can describe the evaluated object more accurately and be further processed to obtain reference information.	The calculation is complicated, and the determination of the index weight vector is subjective. When the index set is large, it is difficult to compare the membership degrees, and even causes the evaluation to fail.
Chaos theory	It can effectively explain or solve nonlinear complex problems, and has obvious effect in short-term prediction.	Chaos behavior is very sensitive to initial conditions, so sufficient and accurate data are required. The effect of long-term prediction is poor.
SVM	It can achieve good performance under less data, and has good generalization performance, which is not easy to over fit.	The speed of large-scale training samples is slow. The traditional SVM is not suitable for multi classification and is sensitive to missing data, parameters, and kernel function.

3.2.6. Intelligent Prediction Models Review

By reading a large number of literature, and extracting and sorting out the information in the literature, 71 intelligent prediction models in Table 5 were finally obtained. Some of these models are basic models, but more of them are hybrid models improving their algorithms, data cleaning methods, and optimizers. The hybrid model often achieves higher accuracy and better performance. These models are sorted as follows according to data size, input variables, output variables, performance, publishing time, etc.

Table 5. 71 intelligent prediction models.

Reference	Model(s)	Data Size (s)	Proportion of Training Set, Validation Set, and Test Set	Input Variable(s)	Output	Performance	Year
[25]	GA-BP	30	2:0:1	OC, pH, TM, P, UL, SC, WC, l , w , d	Burst pressure	MSE = 0.00024659; $R^2 = 0.99988$;	2014
[26]	GBDT	25	4:0:1	SC, pH, TM, UL, P	Corrosion rate	MSE = 0.0000326; MAPE = 0.0225; $R^2 = 0.9834$;	2020
[27]	IABC-EGM (1,1)	18	2:0:1	Elbow wall thickness value	Remaining thickness	MRE = 0.0228;	2021
[28]	RS-PSO-GRNN	20	3:1:1	SR, ORP, pH, SEC, SC	Corrosion rate	RSE = 0.0058; MAPE = 0.0561	2019
[29]	ANN	15	4:0:1	D, WT, UTS, YS, l , d	Remaining thickness	RE;	2016
[30]	PCA-CPSO-SVR	60	0.85:0:0.15	TM, HOL, P, PCO ₂ , UL, TAUWWT, TAUWG, pH	Corrosion rate	MAE = 0.083; RMSE: 0.027; MAPE = 0.166;	2021
[30]	SVR	60	0.85:0:0.15	TM, HOL, P, PCO ₂ , UL, TAUWWT, TAUWG, pH	Corrosion rate	MAE = 0.102; RMSE: 5.9%; MAPE = 0.079;	2021

Table 5. Cont.

Reference	Model(s)	Data Size (s)	Proportion of Training Set, Validation Set, and Test Set	Input Variable(s)	Output	Performance	Year
[30]	PCA-SVR	60	0.85:0:0.15	TM, HOL, P, PCO ₂ , UL, TAUWWT, TAUWG, pH	Corrosion rate	MAE = 0.194; RMSE: 8.1%; MAPE = 0.067;	2021
[30]	PCA-GA-SVR	60	0.85:0:0.15	TM, HOL, P, PCO ₂ , UL, TAUWWT, TAUWG, pH	Corrosion rate	MAE = 0.098; RMSE: 3.1%; MAPE = 0.061;	2021
[30]	PCA-PSO-SVR	60	0.85:0:0.15	TM, HOL, P, PCO ₂ , UL, TAUWWT, TAUWG, pH	Corrosion rate	MAE = 0.083; RMSE: 2.7%; MAPE = 0.053;	2021
[31]	ANN	259	194:0:65	T, DC, PP, WC, pH, BC, RP, SC, BD, SR, CC	Remaining thickness	RMSE = 1.44117; MAE = 1.05954; RMSRE = 1.59692; U ₉₅ = 3.67005; NSE = 0.64576;	2021
[31]	MARS	259	194:0:65	T, DC, PP, WC, pH, BC, RP, SC, BD, SR, CC	Remaining thickness	RMSE = 1.31190; MAE = 0.94897; RMSRE = 1.43685; U ₉₅ = 3.34730; NSE = 0.70646;	2021
[31]	M5Tree	259	194:0:65	T, DC, PP, WC, pH, BC, RP, SC, BD, SR, CC	Remaining thickness	RMSE = 1.39073; MAE = 0.92780; RMSRE = 1.00858 U ₉₅ = 3.52255; NSE = 0.67012;	2021
[31]	LWP	259	194:0:65	T, DC, PP, WC, pH, BC, RP, SC, BD, SR, CC	Remaining thickness	RMSE = 1.60183; MAE = 1.15470; RMSRE = 1.88149; U ₉₅ = 3.90985; NSE = 0.56237;	2021
[31]	KR	259	194:0:65	T, DC, PP, WC, pH, BC, RP, SC, BD, SR, CC	Remaining thickness	RMSE = 1.15683; MAE = 0.90728; RMSRE = 0.98986; U ₉₅ = 3.09315; NSE = 0.77175;	2021
[31]	ELM	259	194:0:65	T, DC, PP, WC, pH, BC, RP, SC, BD, SR, CC	Remaining thickness	RMSE = 1.50760; MAE = 1.12518; RMSRE = 1.51676; U ₉₅ = 3.82753; NSE = 0.61235;	2021
[32]	SSCN	3250	9:0:1	CR, TM, OP, GPR, OPR, WPR, BSW, PCO ₂ , GSG	Corrosion defect depth	MSE = 0.0238;	2020
[32]	DNN	3250	9:0:1	CR, TM, OP, GPR, OPR, WPR, BSW, PCO ₂ , GSG	Corrosion defect depth	MSE = 0.0459	2020
[32]	GBM	3250	9:0:1	CR, TM, OP, GPR, OPR, WPR, BSW, PCO ₂ , GSG	Corrosion defect depth	MSE = 0.0557	2020

Table 5. Cont.

Reference	Model(s)	Data Size (s)	Proportion of Training Set, Validation Set, and Test Set	Input Variable(s)	Output	Performance	Year
[32]	RF	3250	9:0:1	CR, TM, OP, GPR, OPR, WPR, BSW, PCO ₂ , GSG	Corrosion defect depth	MSE = 0.0678	2020
[33]	BWNN-IPSA	30	22:0:8	The six first evaluation indexes I ₁ ~I ₆	The pipeline integrity management level	MSE = 3.16	2021
[33]	FSNN-TDA	30	22:0:8	The six first evaluation indexes I ₁ ~I ₆	The pipeline integrity management level	MSE = 1.38	2021
[33]	FSNN-IDA	30	22:0:8	The six first evaluation indexes I ₁ ~I ₆	The pipeline integrity management level	MSE = 0.79	2021
[34]	ANN	-	-	CR	Corrosion rate	SSE = 0.000010 MSE = 0.000257 MAE = 0.000754 MAPE = 0.12921 MSPE = 6.064%	2012
[34]	Grey forecasting model	-	-	CR	Corrosion rate	SSE = 0.000073 MSE = 0.000710 MAE = 0.001569 MAPE = 0.08772 MSPE = 2.935%	2012
[34]	Stepwise regression forecasting model	-	-	CR	Corrosion rate	SSE = 0.000010 MSE = 0.000261 MAE = 0.000674 MAPE = 0.09612 MSPE = 4.432%	2012
[34]	Combining forecasting model	-	-	CR	Corrosion rate	SSE = 0.000002 MSE = 0.000122 MAE = 0.000191 MAPE = 0.01585 MSPE = 0.637%	2012
[35]	12-inch gas pipelines	1540	8:0:2	T, AW, CC, CP, CG, D, FS, JC, ML, OP, SUP	pipeline condition	R ² = 0.9880 AVP = 0.979 AIP = 0.021 RMSE = 0.008 MAE = 0.098	2014
[35]	20-inch oil pipelines	900	8:0:2	T, AW, CC, CP, CG, D, FS, JC, ML, OP, SUP	pipeline condition	R ² = 0.9940 AVP = 0.962 AIP = 0.038 RMSE = 0.015 MAE = 0.152	2014
[35]	24-inch gas pipelines	2550	8:0:2	T, AW, CC, CP, CG, D, FS, JC, ML, OP, SUP	pipeline condition	R ² = 0.9920 AVP = 0.983 AIP = 0.017 RMSE = 0.005 MAE = 0.079	2014

Table 5. Cont.

Reference	Model(s)	Data Size (s)	Proportion of Training Set, Validation Set, and Test Set	Input Variable(s)	Output	Performance	Year
[35]	Gas pipelines	4990	8:0:2	T, AW, CC, CP, CG, D, FS, JC, ML, OP, SUP	pipeline condition	$R^2 = 0.9910$ AVP = 0.978 AIP = 0.022 RMSE = 0.005 MAE = 0.099	2014
[35]	Oil pipelines	4990	8:0:2	T, AW, CC, CP, CG, D, FS, JC, ML, OP, SUP	pipeline condition	$R^2 = 0.9900$ AVP = 0.979 AIP = 0.021 RMSE = 0.004 MAE = 0.094	2014
[36]	SVM	5	-	HOL, HTK, PSID, USG, TAUWHL, ANGLE, TAUWG	Corrosion rate	11.16% < RE < 25%	2013
[36]	BPNN	5	-	HOL, HTK, PSID, USG, TAUWHL, ANGLE, TAUWG	Corrosion rate	19.54% < RE < 33.33%	2013
[36]	Multiple regression	5	-	HOL, HTK, PSID, USG, TAUWHL, ANGLE, TAUWG	Corrosion rate	25.32% < RE < 44.44%	2013
[37]	MOGWO-SVM	453	9:0:1	D, WT, UTS, YS, EM, BP, l, w, d	Burst pressure	MAE = 0.237; MAPE = 0.01353; RMSE = 0.315; $R^2 = 0.999$; a20-index = 1.000; STDE = 0.276; $\mu = 0.999$	2021
[37]	NSGA-II-SVM	453	9:0:1	D, WT, UTS, YS, EM, BP, l, w, d	Burst pressure	MAE = 0.437; MAPE = 0.03220; RMSE = 0.760; $R^2 = 0.997$; a20-index = 0.978; STDE = 0.731; $\mu = 1.009$	2021
[37]	SVM	453	9:0:1	D, WT, UTS, YS, EM, BP, l, w, d	Burst pressure	MAE = 1.726; MAPE = 0.14987; RMSE = 4.231; $R^2 = 0.735$; a20-index = 0.867; STDE = 4.229; $\mu = 1.109$	2021
[37]	PSO-SVM	453	9:0:1	D, WT, UTS, YS, EM, BP, l, w, d	Burst pressure	MAE = 1.437; MAPE = 0.09772; RMSE = 1.984; $R^2 = 0.986$; a20-index = 0.956; STDE = 1.843; $\mu = 1.018$	2021
[38]	WNN-GA	30	22:0:8	TM, pH, PCO ₂ , CC, BC, SC, CMC	Corrosion rate	RE < 0.032585	2011

Table 5. Cont.

Reference	Model(s)	Data Size (s)	Proportion of Training Set, Validation Set, and Test Set	Input Variable(s)	Output	Performance	Year
[39]	Momentum and adaptive learning rate	294	4:0:1	Pipe size parameters, Material parameters, Defect parameters	Burst pressure	$MSE = 9.8437 \times 10^{-4}$	2011
[39]	Elasticity BP	294	4:0:1	Pipe size parameters, Material parameters, Defect parameters	Burst pressure	$MSE = 7.5571 \times 10^{-6}$	2011
[39]	Levenberg-Marquardt	294	4:0:1	Pipe size parameters, Material parameters, Defect parameters	Burst pressure	$MSE = 1.7521 \times 10^{-10}$	2011
[40]	SGD Regressor	Thousands	3:0:1	WT, T	Remaining thickness	$R^2 = 0.801814$ R^2 -5fold cross validation = 0.79844	2015
[40]	SVM Linear Kernel	Thousands	3:0:1	WT, T	Remaining thickness	$R^2 = 0.785331$ R^2 -5fold cross validation = 0.782201	2015
[40]	SVM Linear Poly Kernel	Thousands	3:0:1	WT, T	Remaining thickness	$R^2 = 0.61937$ R^2 -5fold cross validation = 0.60278	2015
[40]	SVM Linear RBF Kernel	Thousands	3:0:1	WT, T	Remaining thickness	$R^2 = 0.80267$ R^2 -5fold cross validation = 0.79202	2015
[40]	Random Forest	Thousands	3:0:1	WT, T	Remaining thickness	$R^2 = 0.99872$ R^2 -5fold cross validation = 0.96418	2015
[41]	Linear model	15	3:0:2	l, w, d	Burst pressure	$R^2 = 0.8626$, F value = 3.55 DOF = 9 AE = 1.762	2017
[41]	2FI model	15	3:0:2	l, w, d	Burst pressure	$R^2 = 0.9212$, F value = 3.12 DOF = 6 AE = 1.402	2017
[41]	Quadratic model	15	3:0:2	l, w, d	Burst pressure	$R^2 = 0.9577$, F value = 1.53 DOF = 3 AE = 0.095	2017
[42]	GA-BP(L-M)	-	4:0:1	D, WT, YS, CR, d, l	Burst pressure	$MSE = 3.40 \times 10^{-10}$	2013

Table 5. Cont.

Reference	Model(s)	Data Size (s)	Proportion of Training Set, Validation Set, and Test Set	Input Variable(s)	Output	Performance	Year
[43]	PCA-SVR	148	128:0:20	D, WT, YS, CR, d, l	Burst pressure	RMSE = 0.34 MAE = 0.0191	2019
[43]	PCA-GRNN	148	128:0:20	D, WT, YS, CR, d, l	Burst pressure	RMSE = 1.50 MAE = 0.0869	2019
[43]	PCA-WNN	148	128:0:20	D, WT, YS, CR, d, l	Burst pressure	RMSE = 1.25 MAE = 0.0553	2019
[43]	PCA-SVM	148	128:0:20	D, WT, YS, CR, d, l	Burst pressure	RMSE = 1.07 MAE = 0.0671	2019
[44]	PSO-GRNN	60	3:0:1	WC, STC, SR, ORP, SEC, pH, SC, DC;	Corrosion defect depth	RE < 0.1377; MRE = 0.0663;	2019
[45]	RS-PSO-SVM	79	69:0:10	Pipe steel grade, D, WT, d, l	Burst pressure	MAPE = 0.0123; RMSE = 0.17 MPa;	2020
[45]	BPNN	79	69:0:10	Pipe steel grade, D, WT, d, l	Burst pressure	MAPE = 0.0797; RMSE = 1.58 MPa;	2020
[45]	PSO-WNN	79	69:0:10	Pipe steel grade, D, WT, d, l	Burst pressure	MAPE = 0.0596; RMSE = 0.84 MPa;	2020
[46]	DNN	163	114:0:49	l, w, d , Pipeline internal pressure	Maximum equivalent stress	RE = 0.0039; MSE = 0.00054; $R^2 = 0.99607$	2021
[47]	GM-RBF	15	4:0:1	CR	Corrosion rate	MRE = 0.0637; $R^2 = 0.9$	2018
[48]	PSO-SVM	129	109:0:20	Pipe steel grade, D, WT, d, l , YS, UTS	Burst pressure	MRE = 0.01336	2020
[48]	CS-SVM	129	109:0:20	Pipe steel grade, D, WT, d, l , YS, UTS	Burst pressure	MRE = 0.02971	2020
[48]	GA-SVM	129	109:0:20	Pipe steel grade, D, WT, d, l , YS, UTS	Burst pressure	MRE = 0.03344	2020
[48]	CV-SVM	129	109:0:20	Pipe steel grade, D, WT, d, l , YS, UTS	Burst pressure	MRE = 0.03942	2020
[49]	Rlife	105	15:0:6	Transport medium, impurities, oxygen content and others	Remaining thickness	-	2016
[50]	GA-BP	46	4:0:1	$d, l, D, WT, YS, CR;$	Burst pressure	MSE = 0.00612	2015
[51]	PSO-BP	120	105:0:15	l, w, d , axial and circumferential spacing of corrosion defect	Burst pressure	AE = 3.9% RE < 6.4%	2020
[52]	FOA-GRNN	35	30:0:5	D, WT, UTS, w, d, l	Burst pressure	MRE = 7.81%	2020
[53]	GA-BPNNs	39	27:6:6	D, WT, Pipe steel grade, UTS, YS, w, d, l	Burst pressure	-7.78% < RE < 6.06%	2020

4. Discussions

4.1. Publishing Time

Figure 6 shows the number of publications from 2011 to November 2021, for 71 models. Although this is not all the literature, the search results are sorted by relevance, and the data in the figure are still representative and reliable. The figure shows that from 2011 to 2015, the research progress of using intelligent models to predict remaining strength and remaining life was relatively stable. Although there was a sharp decline in 2016–2018, the overall trend was stable. After 2019, related research showed a spurt of growth. It can be inferred that the prediction of remaining strength and remaining life is still a research hot spot.

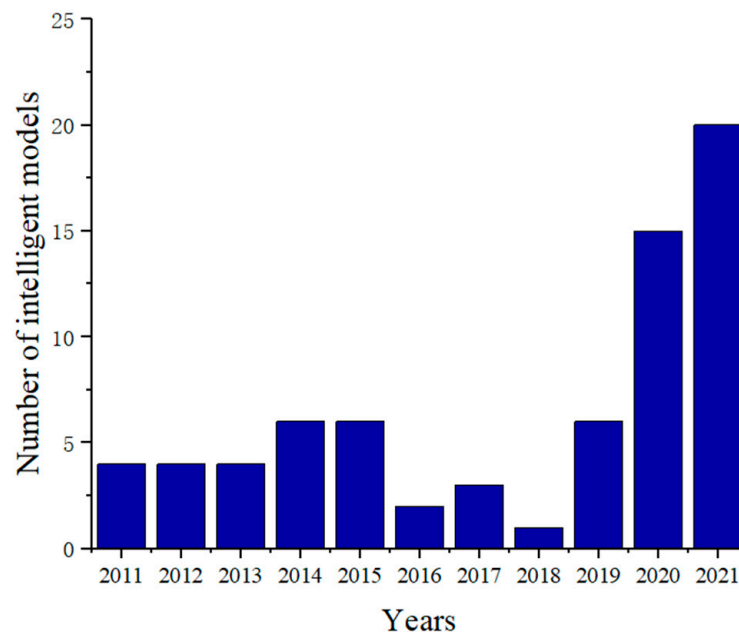


Figure 6. The number of related intelligent models from 2011 to November 2021.

4.2. Result Analysis of Traditional Evaluation Methods

Due to the differences in various evaluation methods in many aspects [54], the calculation results also be affected. In all, 64 groups of data were collected from the literature [12], including 40 groups of low-strength steel grade corrosion pipes (X42, X46-1, X46-2, X46-3, X46-4, X52-1, X52-2, and X56) and 24 groups of medium and high-strength steel grade corrosion pipes (X60, X65, and X80), including defect size parameters, pipe size parameters, material parameters, and burst test pressure. The result analysis of various evaluation methods is shown in Figures 7–10. As the figures show, ASME B31G has large errors in evaluating whether it is a medium-to-high strength pipeline or a low-strength pipeline. The Modified B31G has improved significantly. When evaluating low-strength steel pipes, the DNV-RP-F101 allowable stress method and PCORRC have similar errors. However, when evaluating high-strength steel-grade pipelines, the accuracy of the DNV-RP-F101 allowable stress method is much higher than that of PCORRC.

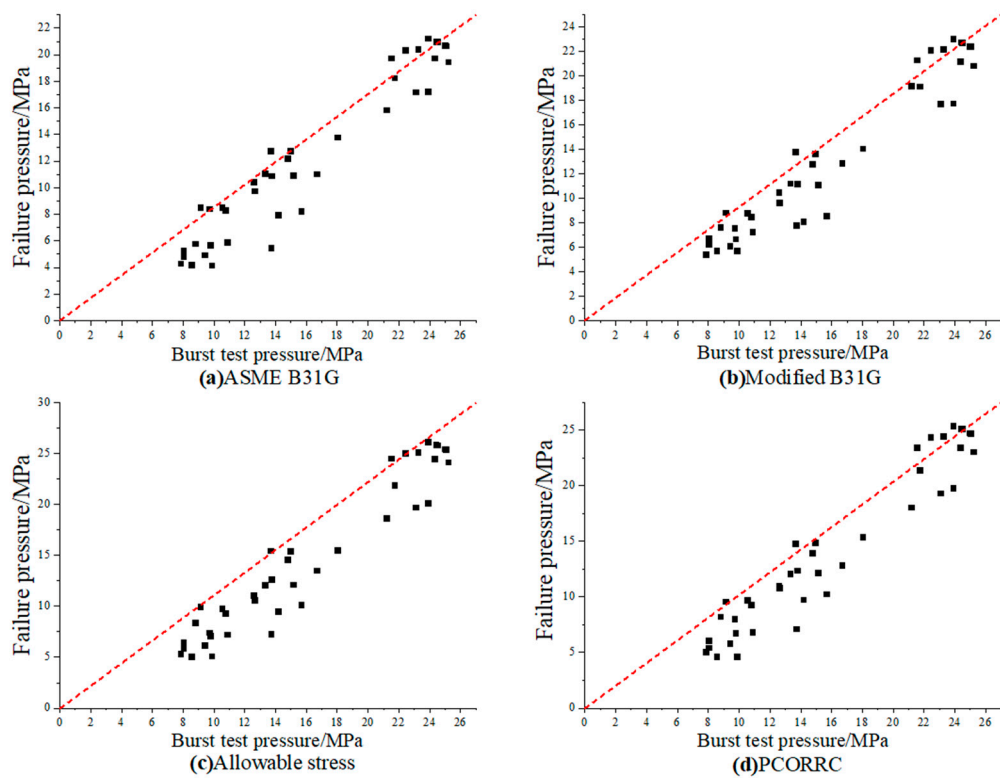


Figure 7. Comparison of burst pressure and predicted failure pressure of low-strength pipelines calculated by different methods: (a) ASME B31G; (b) Modified B31G; (c) Allowable stress; (d) PCORRC.

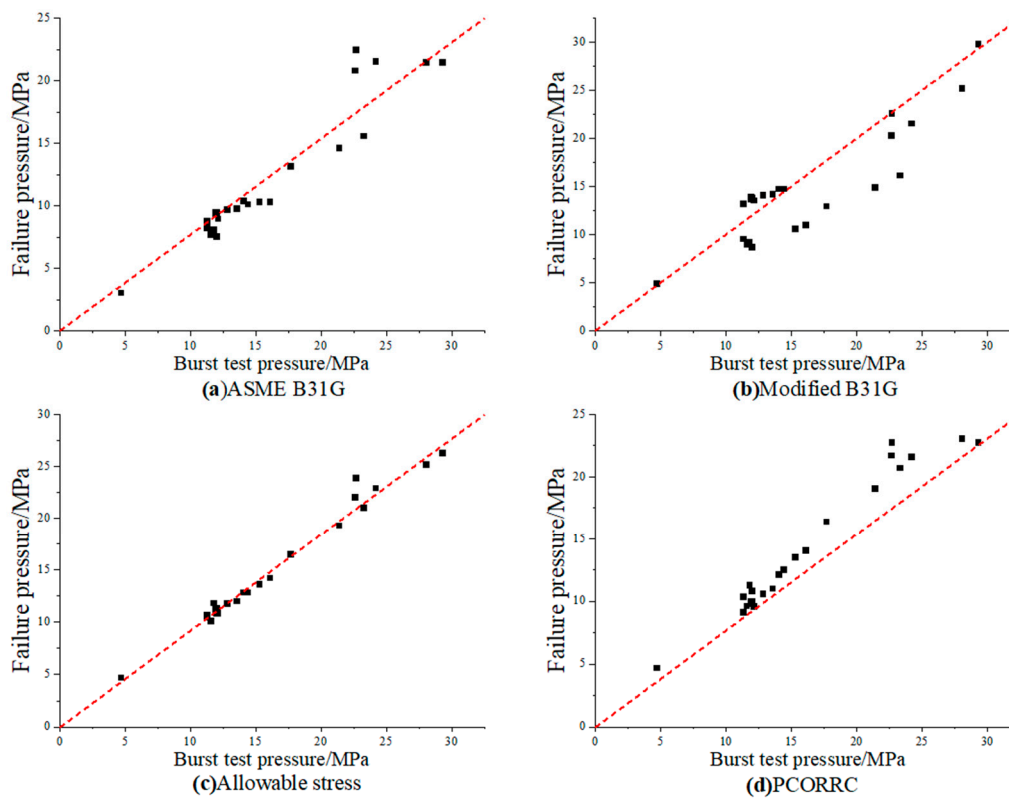


Figure 8. Comparison of burst pressure and predicted failure pressure of medium and high strength pipelines calculated by different methods: (a) ASME B31G; (b) Modified B31G; (c) Allowable stress; (d) PCORRC.

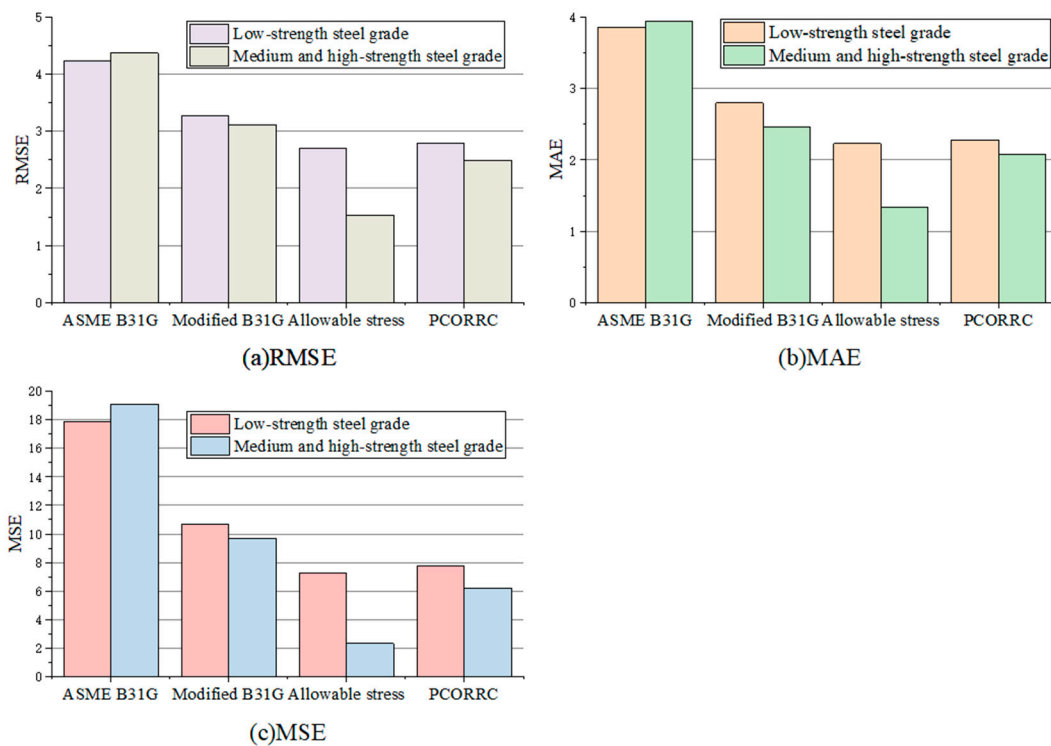


Figure 9. Errors in calculating failure pressure of corroded pipelines of low, medium, and high strength steel grades by different methods: (a) RMSE; (b) MAE; (c) MSE.

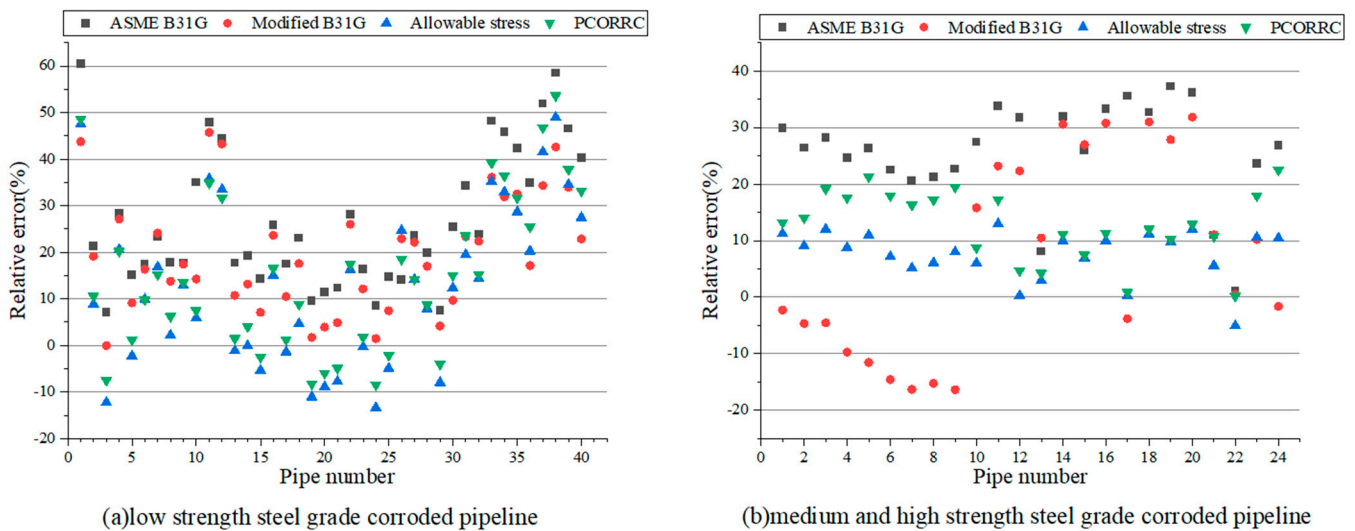


Figure 10. Different methods to calculate relative error of failure pressure of: (a) low-strength steel grade corroded pipeline; (b) high-strength steel grade corroded pipelines.

4.3. Prediction Accuracy

Error indicator can be used to evaluate the performance of prediction model [55–59]. By counting the indicators used in the discussed models, this paper summarizes 18 indicators used to evaluate the prediction accuracy. Their expressions are shown in Equations (28)–(43), Figure 11 indicates that the most frequently used error indicators are MSE, R^2 , MAPE, RMSE, and MAE. Among these indicators, MSE, RMSE, and MAE have no benchmark because the data dimension because the data sets dimensions are different. MAPE and R^2 can be compared in different usage scenarios because they reflect relative errors. The closer R^2 is to one, the higher the prediction accuracy. The smaller the MAPE, the higher the

prediction accuracy. MAPE and R^2 in residual strength and residual life prediction models are counted in the Table 6. Among the 71 models, the range of MAPE is between 0.0123 and 0.1499, the range of R^2 is between 0.619 and 0.999. Lewis once gave a reference, when the MAPE is less than 0.1, the model performance is excellent; when the MAPE is greater than 0.1 and less than 0.2, the model performance is good; when the MAPE is greater than 0.2 and less than 0.5, the model performance is reasonable; and when the MAPE is greater than 0.5, the model is not suitable.

Table 6. MAPE and R2 statistics of residual strength and residual life forecasting results.

Error Indicator	Min.	Max.	Average
MAPE	0.0123	0.1499	0.0708
R2	0.619	0.999	0.833

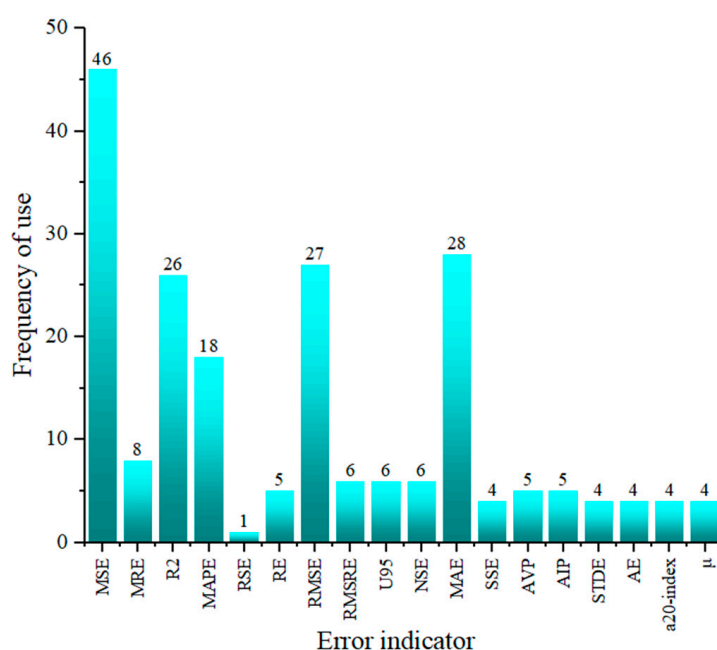


Figure 11. The frequency of using various error indicators in 71 models.

$$MSE = \frac{1}{n} \sum_{i=1}^n (R_i - P_i)^2 \tag{28}$$

$$MRE = \frac{1}{n} \sum_{i=1}^n \left| \frac{R_i - P_i}{R_i} \right| \tag{29}$$

$$RE = \frac{R_i - P_i}{R_i} \tag{30}$$

$$R^2 = 1 - \frac{\sum_{i=1}^n (R_i - P_i)^2}{\sum_{i=1}^n (\bar{R}_i - P_i)^2} \tag{31}$$

$$RMSE = \sqrt{\frac{1}{n} \sum_{i=1}^n (R_i - P_i)^2} \tag{32}$$

$$RMSPE = \sqrt{\frac{1}{n} \sum_{i=1}^n \left(\frac{R_i - P_i}{R_i} \right)^2} \tag{33}$$

$$U_{95} = 1.96 \sqrt{\frac{\sum_{i=1}^n (R_i - \bar{R})}{n - 1} - \frac{\sum_{i=1}^n (R_i - P_i)^2}{n}} \tag{34}$$

$$NSE = 1 - \frac{\sum_{i=1}^n (R_i - P_i)^2}{\sum_{i=1}^n (R_i - \overline{R_i})^2} \quad (35)$$

$$MAE = \frac{1}{n} \sum_{i=1}^n |R_i - P_i| \quad (36)$$

$$SSE = \sum_{i=1}^n (R_i - P_i)^2 \quad (37)$$

$$AIP = \frac{100\%}{n} \sum_{i=1}^n \left| 1 - \frac{P_i}{R_i} \right| \quad (38)$$

$$AVP = 1 - AIP \quad (39)$$

$$STDE = std(R_i - P_i) \quad (40)$$

$$AE = |R_i - P_i| \quad (41)$$

$$a20 - index = \frac{er20}{n} \quad (42)$$

$$\mu = \frac{1}{n} \sum_{i=1}^n \frac{P_i}{R_i} \quad (43)$$

4.4. Data Size and Data Division

Data size is one of the main factors affecting forecasting performance. Too much data will lead to too much calculation, while too little data may lead to the insufficient model accuracy. Table 7 provides statistical information on the data size of 71 smart models, which can provide a basis for selecting data sizes in subsequent studies. The original data are usually divided into three data sets in machine learning, including training set, validation set, and test set. The training set is used to train the model; the validation set data are used to adjust the parameters of the training model; and the test set data are used to measure the performance of the training model. However, only 2 of the 71 models divide the original data into three data sets, and the remaining 69 models only divide it into the training and test sets (Figure 12). The proportion of test set is in the range of 0.015–0.4.

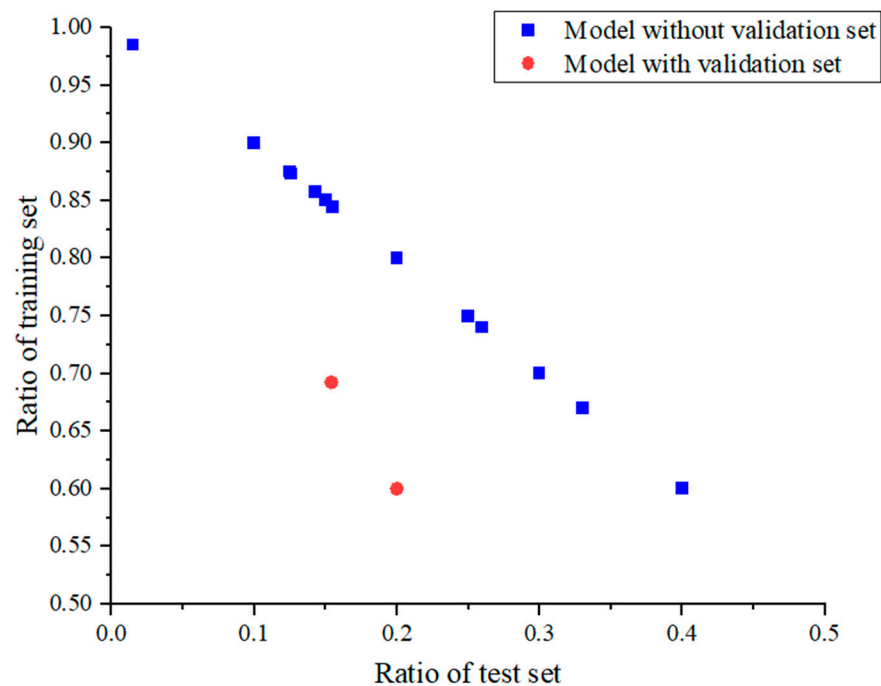


Figure 12. Division proportion of raw data.

Table 7. The data size of prediction models.

Burst Pressure			Remaining Thickness			Corrosion Rate			Corrosion Defect Depth			Others		
Max.	Min.	Mean	Max.	Min.	Mean	Max.	Min.	Mean	Max.	Min.	Mean	Max.	Min.	Mean
453	15	167	259	15	188	60	15	43	3250	60	2612	4990	30	2171

4.5. Input Variable and Output Value

In the intelligent model, how to determine the input variables is a very critical issue [60,61]. Therefore, in the remaining strength and remaining life prediction model, it is necessary to consider which factors are used as input variables fully. According to the input variables, it can be divided into two categories. One is to simply use certain historical data as input variables to predict the future trend of the variable, such as using the historical wall thickness of the pipeline to predict the remaining wall thickness or using the historical corrosion rate to predict the future corrosion rate. The other is the prediction that considers multiple factors, such as predicting the burst pressure of the pipeline through pipeline size parameters, defect parameters, environmental parameters, and material parameters (Table 8). The former is simple to calculate, and convenient to obtain data, but the prediction accuracy is not necessarily high, because this type of prediction assumes that external factors are stable. The latter is difficult to obtain data, and needs to consider the nonlinear relationship of multiple variables, but the prediction results are often more comprehensive and accurate. According to the statics of the models compiled in this paper, 10 of the 71 models are simple time-series predictions, and the rest are forecasting considering multiple factors.

Table 8. The input variables of prediction models.

Input Variables Type	Parameters
Environmental factor	P, UL, TM, SR, ORP, PCO ₂ , TAUWWT, TAUWG, PP, RP, BD, CC, OP, BSW, GSG, GPR, OPR, WPR, AW, CP, CG, JC, FS, ML, SUP, HTK, USG, BP, EM, STC, OC, pH, SC, WC, SEC, HOL, DC, BC, CMC, SEC
Corrosion Defect data	<i>l, w, d</i>
Pipe data	D, WT
Material	UTS, YS, TS, EM, BP, Pipe steel grade
Others	T, CR

The prediction targets of these models can be roughly divided into the following four categories: burst pressure, remaining thickness, corrosion rate, and others. Among them, burst pressure accounts for 36%, remaining thickness accounts for 18.7%, corrosion rate accounts for 21.3%, corrosion defect depth accounts for 6.7%, and the others accounts for 17.3%. The proportion of each item is shown in Figure 13. It can be seen from Figure 13 that the model with burst pressure as the output value is still the most, the rest are similar.

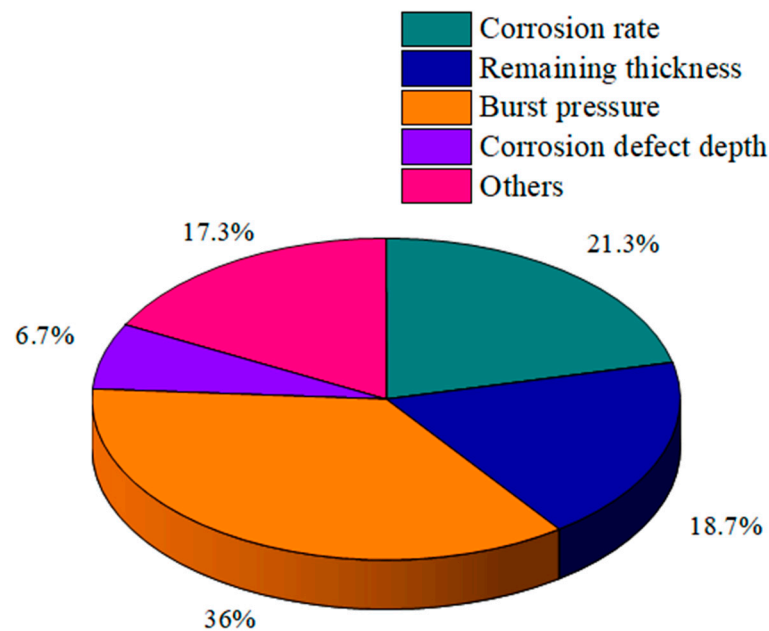


Figure 13. Output value of 71 models.

4.6. Future Research Directions

Based on the literature review, the future development direction of the residual strength and residual life prediction models is summarized as follows:

1. Most models ignore setting the validation set. In fact, in machine learning, adjusting parameters can effectively improve the prediction performance of the model.
2. Many of the existing models have achieved good accuracy, but few papers mention the stability of these models. If these models are needed to be used in actual working conditions, stability is also important.
3. Existing models usually have small amounts of data collected, leading to limitations in their predictions. More efforts can be made in data collection to improve their generality.
4. At present, most studies are mainly based on uniform corrosion under normal conditions, but do not consider the degradation of pipeline materials, in fact, the change in mechanical characteristics can be very large, while the kinetics of degradation of mechanical properties differs in different climatic zones [62,63]. More specific conditions can be considered for further research in the future.

5. Conclusions

This paper reviews the assessment of pipeline residual strength and residual life prediction works from 2009 to November 2021. After screening, a total of 71 models are carefully reviewed. The parameters, application scope, defect type, load type, and accuracy of the traditional evaluation methods are compared, but publishing time, prediction accuracy, data size, data division, input variable, and output value are further discussed. Based on the analysis and discussion results, the following primary conclusions can be drawn:

1. In the past ten years, from 2011 to 2018, the research progress of remaining strength and remaining life has been relatively stable and the number increased significantly after 2018. The improved hybrid model based on the basic model is a research hotspot. Furthermore, predicting with improved intelligent models will be the trend in the future.
2. The accuracy of Modified B31G is higher than ASME B31G, but it is not suitable to evaluate medium–high strength steel grades pipelines. PCORRC and DNV-RP-

- F101 are similar in evaluating low strength pipelines, and DNV-RP-F101 has a better performance in evaluating medium–high strength pipelines.
3. The most frequently used error indicators are MSE, R2, MAPE, RMSE, and MAE. Among them, MAPE is in the range of 0.0123–0.1499; R2 is in the range of 0.619–0.999.
 4. The proportion of test data set is between 0.015 and 0.4, and only 2 of 71 models are using the validation set. In fact, correctly setting the proportion of data can further improve the prediction accuracy and achieve better results. Researchers also need to pay more attention to this aspect.
 5. Models are divided into considering a single variable in the time series, and considering multiple factors based on input variables. There are 61 of 71 models in this paper considering multiple factors. These models can be divided into four main categories based on output value. Among them, burst pressure accounts for 36%, remaining thickness accounts for 18.7%, corrosion rate accounts for 21.3%, corrosion defect depth accounts for 6.7%, and the others accounts for 17.3%.

Author Contributions: Conceptualization, H.L.; formal analysis, H.L.; investigation, H.L.; resources, Q.Z.; writing—original draft preparation, H.L.; writing—review and editing, K.H.; visualization, C.S.; supervision, K.H. All authors have read and agreed to the published version of the manuscript.

Funding: This research received no external funding.

Institutional Review Board Statement: Not applicable.

Informed Consent Statement: Not applicable.

Data Availability Statement: Not applicable.

Acknowledgments: Thanks to Lu Hongfang for his careful guidance during the writing of the thesis.

Conflicts of Interest: The authors declare no conflict of interest.

Nomenclature

A	Projected area of defect on axial through wall plane
A^*	The triangular fuzzy number
A_0	Cross sectional area of original pipe wall at defect
a20-index	er20/n
er20	Number of samples whose absolute error is less than 20%
M	Folias Bulging Coefficient
n	Sample size
f_u	Tensile strength (considering temperature reduction effect)
P_f	The residual strength of the pipe
P_i	Prediction value at time k
R^2	Goodness of Fit
R_i	Real value at time i
std	Population standard deviation
U_{95}	The confidence level of the expanded uncertainty is 95%
σ_{flow}	The flow stress
σ_u	The tensile strength of the pipe
ε_d	Quantile coefficient of defect depth
γ_m	Partial safety factor
γ_d	Defect depth safety factor
$(d/t)^*$	$(d/t)_{meas} + \varepsilon_d \cdot std(d/t)$
$(d/t)_{meas}$	Measured value of defect depth ratio

Abbreviations

AE	Average Error
AGA	American National Gas Association
AIP	Average Invalidity Percent
ANN	Artificial Neural Network
ANP	Analytic Network Process

ASME	American Society of Mechanical Engineers
AVP	Average Validity Percent
AW	Anode Wastage
BC	Bicarbonate
BD	Bulk Density
BG	British Gas Company
BP	Burst Pressure
BPNN	Back Propagation Neural Network
BSW	Basic Sediments and Water
BWNN	B-spline Wavelet Neural Network
CC	Coating Condition
CDD	Corrosion Defect Depth
CG	Crossings
CMC	Calcium/Magnesium ion Content
CP	Cathodic Protection
CR	Corrosion Rate
CS	Cuckoo Search
CV	Cross Validation
d	The depth of corrosion defect
D	Pipe Diameter
DC	Dissolved Chloride
DNN	Deep Neural Networks
DNV	DET NORSKE VERITAS
EGIG	European Gas Pipeline Incident Data Group
ELM	Extreme Learning Machines
EM	Elastic Modulus
FS	Free Spans
FSM	Field Signature Method
FSNN	Fuzzy Surfacelet Neural Network
GA	Genetic Algorithm
GBDT	Gradient Boosting Decision Tree
GBM	Gradient Boosting Machine
GM(1,1)	First Order Univariate Gray System Model
GPR	Gas Production Rate
GRNN	General Regression Neural Network
GSG	Gas Specific Gravity
HOL	Liquid Holdup
HTK	Heat Transfer Coefficient of Inner wall
IDA	Improved Dragonfly Algorithm
IPSA	Improved Particle Swarm Algorithm
JC	Joint Condition
KR	Kriging
l	the length of corrosion defect
LWP	Locally Weighted Polynomials
MAE	Mean Absolute Error
MAPE	Mean Absolute Percentage Error
MARS	Multivariate Adaptive Regression Splines
ML	Metal Loss
MOGWO	Multiobjective Grey Wolf Optimization
MRE	Mean Relative Error
MSE	Mean Square Error
NSE	Nash-Sutcliffe Efficiency
NSGA	Nondominated Sorting Genetic Algorithm
OC	Oxygen Content
OP	Operating Pressure
OPR	Oil Production Rate
ORP	Oxidation-reduction potential
P	Pressure

PCA	Principal Component Analysis
PCO ₂	Partial Pressure of CO ₂
PCORRC	Pipeline Corrosion Criterion
PP	Pipe-to-soil Potential
PSID	Deposition Rate
PSO	Particle Swarm Optimization
PSO	Particle Swarm Optimizer
RBF	Radial Basis Function
RE	Relative Error
RF	Random Forest
RMSE	Root Mean Square Error
RMSRE	Root Mean Squared Relative Error
RP	Redox Potential
RS	Rough Set
SC	Sulfate ion Concentrations
SEC	Stray Electric Current
SGD	Stochastic Gradient Descent
SR	Soil resistivity
SSCN	Subspace Clustered Neural Network
SSE	Error Sum of Squares
SMTS	The material tensile limit
SMYS	The minimum yield stress
STC	Salt Content
STDE	Population standard deviation of error
SUP	Support Condition
SVM	Support Vector Machine
SVR	Support Vector Regression
T	Time(years)
TAUWG	Wall shear stress (gas phase)
TAUWHL	Liquid-maximum wall shear stress
TAUWWT	Wall shear stress (liquid phase)
TDA	Traditional Dragonfly Algorithm
TM	Temperature
UL	Liquid flow rate
USG	Superficial Velocity Gas
UTS	Ultimate Tensile Strength
<i>w</i>	The width of corrosion defect
WC	Water Content
WNN	Weighted nearest neighbor
WPR	Water Production Rate
WT	Wall Thickness
YS	Yield Strength

References

1. EGIG. Available online: <https://www.egig.eu/reports> (accessed on 19 October 2021).
2. Lyons, C.J.; Race, J.M.; Chang, E.; Cosham, A.; Barnett, J. Validation of the ng-18 equations for thick walled pipelines. *EFA* **2020**, *112*, 104494. [[CrossRef](#)]
3. The American Society of Mechanical Engineers. *Manual for Determining the Remaining Strength of Corroded Pipelines*; ASME: New York, NY, USA, 1984; pp. 1–38.
4. The American Society of Mechanical Engineers. *Manual for Determining the Remaining Strength of Corroded Pipelines*; ASME: New York, NY, USA, 1991; pp. 1–47.
5. Kiefner, J.F.; Vieth, P.H. *A Modified Criterion for Evaluating the Remaining Strength of Corroded Pipe*; Pipeline Research Committee, American Gas Association: Washington, DC, USA, 1989.
6. Ma, B.; Jian, S.; Wang, J.; Han, K. Analysis on the latest assessment criteria of ASME b31g-2009 for the remaining strength of corroded pipelines. *JFAP* **2011**, *11*, 666–671. [[CrossRef](#)]
7. Ma, B.; Shuai, J.; Li, X.; Wang, J.; Feng, Q. Advances in the newest version of ASME b31g-2009. *NGI* **2011**, *31*, 112–115.
8. Veritas, D.N. Corroded Pipelines; RP, 2004; p. 11. Available online: http://opimsoft.com/download/reference/rp-f101_2006-10.pdf (accessed on 19 October 2021).

9. Xiao, K.; Liu, Y.; Wang, L.; Qian, Y. *A Study on Assessment Methods for the Remaining Strength of Corroded Pipelines*; GCI: Anchorage, AK, USA, 2013.
10. Stephens, D.R.; Leis, B.N.; Kurre, M.D.; Rudland, D.L. Development of an alternative criterion for residual strength of corrosion defects in moderate-to high-toughness pipe. In Proceedings of the 2000 International Pipeline Conference, Calgary, AB, Canada, 1–5 October 2000.
11. Tomar, M.S.; Fingerhut, M. Reliable application of rstreng criteria for in-the-ditch assessment of corrosion defects in transmission pipelines. *NACE Int. Corros. Conf. Ser.* **2006**, *176*, 1–8.
12. Wang, L.B. Development of Software for Residual Strength Evaluation and Residual Life Prediction of Corroded Pipelines. Master's Thesis, Xi'an Shiyou University, Xi'an, China, 2014.
13. Hua, C. Contrastive Study on New and Old Evaluation Standards of SY/T 6151 for Corrosion Pipeline. *CCI* **2016**, *45*, 1476–1479.
14. Chen, Z.; Wu, M.; Xie, F.; Wang, D.; Guo, Q.; Ma, F. Evaluation method and remaining life prediction of corroded pipeline residual strength. *MEM* **2015**, *5*, 97–101.
15. Rosenblatt, F. The perceptron: A probabilistic model for information storage and organization in the brain. *Psychol. Rev.* **1958**, *65*, 386–408. [[CrossRef](#)] [[PubMed](#)]
16. Katz, W.T.; Snell, J.W.; Merickel, M.B. Artificial neural networks. *Methods Enzymol.* **1992**, *210*, 610–636.
17. Rahmanifard, H.; Plaksina, T. Application of artificial intelligence techniques in the petroleum industry: A review. *Artif. Intell. Rev.* **2019**, *52*, 2295–2318. [[CrossRef](#)]
18. Zhao, Y.; Zhao, B. Research on pressure pipeline explosion based on triangular fuzzy mathematics and fault tree analysis. *JLUPCT* **2018**, *6*, 65–69.
19. Wind, Y.; Saaty, T. Marketing Applications of the Analytic Hierarchy Process. *Manag. Sci.* **1980**, *26*, 641–658. [[CrossRef](#)]
20. Liang, Q. Pressure pipeline leakage risk research based on trapezoidal membership degree fuzzy mathematics. *GST* **2019**, *24*, 48–53.
21. Lorenz, E.N. Deterministic nonperiodic flow. *SNY* **1963**, *20*, 130–141. [[CrossRef](#)]
22. Hunt, B.R.; Li, T.Y.; Kennedy, J.A.; Nusse, H.E. Period three implies chaos. *SNY* **2004**, *6*, 77–84.
23. Cortes, C.; Vapnik, V.; Llorens, C. Support-vector networks. *Mach. Learn.* **1995**, *20*, 273–297. [[CrossRef](#)]
24. Liu, H.; Liu, D.; Zheng, G.; Liang, Y. Research on natural gas short term load forecasting based on support vector expression. *Chin. J. Chem. Eng.* **2004**, *12*, 5.
25. Qu, C. Study on Residual Life Prediction METHOD of Corrosive Defective Pipeline. Master's Thesis, Northeast University, Shenyang, China, 2014.
26. Yan, J. Study on Prediction and Evaluation Method of Inner WALL corrosion of SUBMARINE pipeline. Master's Thesis, Dalian University of Technology, Dalian, China, 2020.
27. Qin, X.; Liu, W.; Chen, L. Pipeline corrosion prediction based on improved bee colony algorithm and grey model. *J. Beijing Univ. Chem. Technol.* **2021**, *48*, 74–80.
28. Wang, W.H. Corrosion Rate Prediction and Residual Life Research of Buried Oil and Gas Pipelines. Master's Thesis, Xi'an University of Architecture and Technology, Xi'an, China, 2019.
29. Cheng, X. Study on Corrosion Residual Life Prediction of Buried Gas PIPELINE Based on Comprehensive Detection. Master's Thesis, South China University of Technology, Guangzhou, China, 2016.
30. Peng, S.; Zhang, Z.; Liu, E.; Liu, W.; Qiao, W. A new hybrid algorithm model for prediction of internal corrosion rate of multiphase pipeline. *J. Nat. Gas. Sci. Eng.* **2021**, *85*, 103716. [[CrossRef](#)]
31. Ben Seghier, M.E.A.; Keshtegar, B.; Taleb-Berrouane, M.; Abbassi, R.; Trung, N. Advanced intelligence frameworks for predicting maximum pitting corrosion depth in oil and gas pipelines. *Process Saf. Environ.* **2021**, *147*, 818–833. [[CrossRef](#)]
32. Ossai, C.I. Corrosion defect modelling of aged pipelines with a feed-forward multi-layer neural network for leak and burst failure estimation. *Eng. Fail. Anal.* **2020**, *110*, 104397. [[CrossRef](#)]
33. Sun, J.; Zhao, B.; Gao, D.; Xu, L. Fuzzy surfacelet neural network evaluation model optimized by adaptive dragonfly algorithm for pipeline network integrity management. *Appl. Soft. Comput.* **2021**, *113*, 107862. [[CrossRef](#)]
34. Zhang, T.; Zhou, L. Combining Forecasting Model of Pipeline's Corrosion Rate Based on Artificial Immune Algorithm. In Proceedings of the International Conference on Pipelines and Trenchless, Wuhan, China, 19–22 October 2012.
35. El-Abbasy, M.S.; Senouci, A.; Zayed, T.; Mirahadi, F.; Parvizsedghy, L. Condition Prediction Models for Oil and Gas Pipelines Using Regression Analysis. *J. Constr. Eng. Manag.* **2014**, *140*. [[CrossRef](#)]
36. Luo, Z.; Hu, X.; Gao, Y. Corrosion research of wet natural gathering and transportation pipeline based on SVM. In Proceedings of the International Conference on Pipelines and Trenchless, Xi'an, China, 16–18 October 2013.
37. Lu, H.; Xu, Z.D.; Iseley, T.; Matthews, J.C. Novel Data-Driven Framework for Predicting Residual Strength of Corroded Pipelines. *J. Pipeline Syst. Eng.* **2021**, *12*, 04021045. [[CrossRef](#)]
38. Zheng, Y.; Shu, J.; Ren, C.; Zhang, F. Prediction of Gathering Pipeline Internal Corrosion Rate Based on Improved Wavelet Neural Network Model. In Proceedings of the International Conference on Pipelines and Trenchless Technology, Beijing, China, 26–29 October 2011.
39. Sun, B.C.; Li, S.X.; Yu, S.R.; Zeng, H.L. Improved BP algorithm to predict the residual strength of corroded pipelines. *CJCP* **2011**, *5*, 404–408.

40. Sharifi, M.; Yao, K.T.; Raghavendra, S.; Ershaghi, I.; House, R.; Blouin, J. Prediction of Remaining Life in Pipes using Machine Learning from Thickness Measurements. In Proceedings of the SPE Western Regional Meeting, Garden Grove, CA, USA, 27–30 April 2015.
41. Hou, P.P. Research on the Influence of Corrosion Defects on the Residual Strength of Oil and Gas Pipelines. Master's Thesis, Xinjiang University, Xinjiang, China, 2017.
42. Sun, B.C.; Wu, J.W.; Li, L.; She, Z.G. Improved GA-BP algorithm for oil and gas pipeline corrosion residual strength prediction. *JSPU Nat. Sci. Ed.* **2013**, *3*, 160–167.
43. Ma, S.; Li, J.F.; Bai, R.; Dai, Z. Prediction of residual strength of oil and gas pipelines based on PCA-SVR model. *OGST* **2019**, *10*, 1119–1124.
44. Wang, W.H.; Luo, Z.S.; Zhang, X.S. Prediction of buried pipeline corrosion remaining life based on PSO-GRNN model. *Surf. Technol.* **2019**, *10*, 267–275.
45. Yang, X.D.; Zhou, Y.L.; Liu, Z.J.; Lu, L.; Yu, T.Q.; Liu, Y. Research on residual strength prediction technology of corroded pipeline based on RS-PSO-SVM algorithm. *PEC* **2020**, *3*, 8–12.
46. Xie, P.; Liu, H.; Gong, Y.H.; Ni, P.P.; Heman, A. Evaluation of residual strength of external corrosion of submarine pipelines based on deep learning. *OGST* **2021**, *6*, 651–657.
47. Luo, Z.S.; Yuan, H.W. GM-RBF submarine pipeline corrosion prediction model based on error compensation. *CJSS* **2018**, *3*, 96–101.
48. Ma, G. Residual Strength Prediction of Single-Defect Pipeline Based on Correlation Analysis and SVM Algorithm. Master's Thesis, Xi'an Petroleum University, Xi'an, China, 2020.
49. Li, J.G.; Lin, S.J.; Long, W.; Xu, L. Prediction of remaining life of metal pipes in uniform corrosion based on FSM non-destructive testing. *Surf. Technol.* **2016**, *3*, 7–11.
50. Li, Q.; Sun, C.M.; Huang, Z.Q.; Xiao, X.; Tang, H.P. Combined forecasting method of GA-BP neural network for failure pressure of Lan-Cheng-Yu corroded pipelines. *OJSST* **2015**, *11*, 83–89.
51. Zhang, Y. Research on Residual Strength of Multipoint Corrosion Defective Pipeline Based on Finite Element and PSO-BP. Master's Thesis, Xi'an University of Architecture and Technology, Xi'an, China, 2020.
52. Bi, A.R.; Luo, Z.S.; Song, Y.Y.; Zhang, X.S. Residual strength analysis of internally corroded submarine pipeline based on FOA-GRNN model. *CSSJ* **2020**, *6*, 78–83.
53. Jia, S.Q.; Qie, Y.H.; Li, Y.T.; Li, N.N. Research on burst pressure prediction of oil and gas pipelines with uniform corrosion defects based on GA-BPNNs algorithm. *JSST* **2020**, *12*, 105–110.
54. Syrotyuk, A.; Vytyaz, O.; Ziaja, J. Damage to flexible pipes of coiled tubing equipment due to corrosion and fatigue: Methods and approaches for evaluation. *Min. Mineral. Depos.* **2017**, *11*, 96–103. [[CrossRef](#)]
55. Lu, H.; Iseley, T.; Matthews, J.; Liao, W.; Azimi, M. An ensemble model based on relevance vector machine and multi-objective salp swarm algorithm for predicting burst pressure of corroded pipelines. *J. Petrol. Sci. Eng.* **2021**, *203*, 108585. [[CrossRef](#)]
56. Xu, Z.D.; Zhu, C.; Shao, L.W. Damage identification of pipeline based on ultrasonic guided wave and wavelet denoising. *J. Pipeline Syst. Eng.* **2021**, *12*, 04021051. [[CrossRef](#)]
57. Lu, H.; Iseley, T.; Matthews, J.; Liao, W. Hybrid machine learning for pullback force forecasting during horizontal directional drilling. *Automat. Constr.* **2021**, *129*, 103810. [[CrossRef](#)]
58. Xu, Z.D.; Yang, Y.; Miao, A.N. Dynamic Analysis and Parameter Optimization of Pipelines with Multidimensional Vibration Isolation and Mitigation Device. *J. Pipeline Syst. Eng.* **2021**, *12*, 04020058. [[CrossRef](#)]
59. Lu, H.; Matthews, J.C.; Azimi, M.; Iseley, T. Near Real-Time HDD Pullback Force Prediction Model Based on Improved Radial Basis Function Neural Networks. *J. Pipeline Syst. Eng.* **2020**, *11*, 04020042. [[CrossRef](#)]
60. Peng, S.; Chen, R.; Yu, B.; Xiang, M.; Lin, X.; Liu, E.E. Daily natural gas load forecasting based on the combination of long short term memory, local mean decomposition, and wavelet threshold denoising algorithm. *J. Nat. Gas. Sci. Eng.* **2021**, *95*, 104175. [[CrossRef](#)]
61. Lu, H.; Behbahani, S.; Ma, X.; Iseley, T. A multi-objective optimizer-based model for predicting composite material properties. *Constr. Build. Mater.* **2021**, *284*, 122746. [[CrossRef](#)]
62. Maruschak, P.; Prentkovskis, O.; Bishchak, R. Defectiveness of external and internal surfaces of the main oil and gas pipelines after long-term operation. *J. Civil. Eng. Manag.* **2016**, *22*, 279–286. [[CrossRef](#)]
63. Panin, S.; Maruschak, P.; Vlasov, I.; Syromyatnikova, A.; Bolshakov, A.; Berto, F.; Prentkovskis, O.; Ovechkin, B. Effect of Operating Degradation in Arctic Conditions on Physical and Mechanical Properties of 09Mn2Si Pipeline Steel. *Procedia Eng.* **2017**, *178*, 597–603. [[CrossRef](#)]